IOP Conf. Series: Journal of Physics: Conf. Series **1092** (2018) 012031 doi:10.1088/1742-6596/1092/1/012031

Multi-functional RF coils for ultra-high field MRI based on 1D/2D electromagnetic metamaterials

Daniel Erni [1,2], Andreas Rennings [1], Jan Taro Svejda [1], Benedikt Sievert [1], Zhichao Chen [1], Thorsten Liebig [1], Juerg Froehlich [1,2,3]

[1] General and Theoretical Electrical Engineering (ATE), Faculty of Engineering, and CENIDE – Center for Nanointegration Duisburg-Essen, University of Duisburg-Essen, D-47048 Duisburg, Germany.

[2] Institute of Electromagnetic Fields (IEF), Department of Information Technology and Electrical Engineering, ETH Zürich, CH-8092 Zürich, Switzerland.

[3] Fields at Work GmbH, CH-8006 Zürich, Switzerland.

E-mail: daniel.erni@uni-due.de

Abstract. Electromagnetic metamaterials have already proven very valuable for the enhancement and molding of RF magnetic fields within ultra-high field MRI scanners at 7T. We report on our development of coil elements based on composite right-/left-handed (CRLH) 1D electromagnetic (EM) metamaterial transmission lines (*metalines*) operating in the zeroth order resonance (ZOR) to foster uniform RF magnetic field distributions along the scanner axis. Tailored EM metalines supporting full-wave or quarter-wave resonances are used either as metamaterial ring antenna or as dual-band coil elements for simultaneous ^{1}H/^{23}Na imaging. The EM metalines are key to the *MetaBore*, which is a fully adaptive RF field control scheme based on a periodic axial arrangement of conformal metamaterial ring antennas in the framework of high-field traveling-wave MRI. With the 2D EM metamaterials (*metasurfaces*) we realized high-impedance surfaces (HIS) in order to enhance the uniformity and directivity of the RF magnetic field from e.g. overlaid (elongated) dipole elements towards the probe volume. The designs include simulation studies of the overall multichannel coil systems, which are carried out with our home-made, open source electromagnetic 3D EC-FDTD solver *openEMS* supporting conformal cylindrical inhomogeneous meshing. Experimental verifications of our coils have been carried out within 7T MRI scanners (Siemens Magnetom).

1. Introduction

Since the seminal proposal of V. G. Veselago [1] in 1968, where for the first time the potential of properly tailoring electromagnetic (EM) material parameters had been laid out, electromagnetic metamaterials (MTMs) have evolved into one of the most powerful paradigms of modern engineering science. The possibility for dispersion engineering and meta-doping (e.g. the introduction resonant and radiative defects) has led to various novel EM applications encompassing e.g. compact leaky wave antennas, real-time analog signal processing, functional meta-surfaces for e.g. (spatial) transformation optics/electromagnetics, and miniaturized multi-functional metadevices [2] while covering most of the EM spectrum. The application of EM MTMs in ultra-high field (UHF) magnetic resonance imaging (MRI) has started midst of the noughties where mainly the lensing capabilities of MTM pads have been exploited for enhancing the B_1 efficiency in e.g. extremities. Although boosting MRI sensitivity

via e.g. MTM surfaces (*metasurfaces*) has now improved into a mature technology [3], proper MTM-based coil designs for UHF MRI have only emerged in the wake of utilizing composite right-/left-handed (CRLH) MTM transmission lines (*metalines*) in modern RF engineering [4-7]. In the remainder of the paper we shall briefly summarize part of our research on the use of CRLH metalines in multi-functional coil design [4-13] for UHF MRI at 7T as well as on the field enhancement due to a HIS metasurface within an 8-channel coil design using optimized elongated dipole elements [15-16].

2. Coils based on CRLH metamaterial transmission lines (metalines)

2.1. Zeroth order resonance (ZOR) coil elements for 7T MRI

A common element in coil design based on CRLH metalines lies in the applicability of dispersion engineering as an additional degree-of-freedom. In coil elements operating in the zeroth order resonance (ZOR) the resulting uniform current (and $\boldsymbol{B}_1$ field) distribution (cf. figure 1) has been exploited for providing large longitudinal field of views (FoVs) [4, 5] up to 40cm [6] that are virtually scalable with the number of unit cells. A 4-channel coil design with frequency balanced CRLH unit cells [6, 7] yielded $|\boldsymbol{B}_1^+|_{max}/(SAR_{max})^{0.5} = -2.6$dB, an inter-element coupling $S_{ij} \leq -30$dB and a $SAR_{10g} \sim 70\%$ (cf. to microstrip dipole element) within an uniform octogonal phantom (where $|\boldsymbol{E}|^2$ directly maps to SAR).

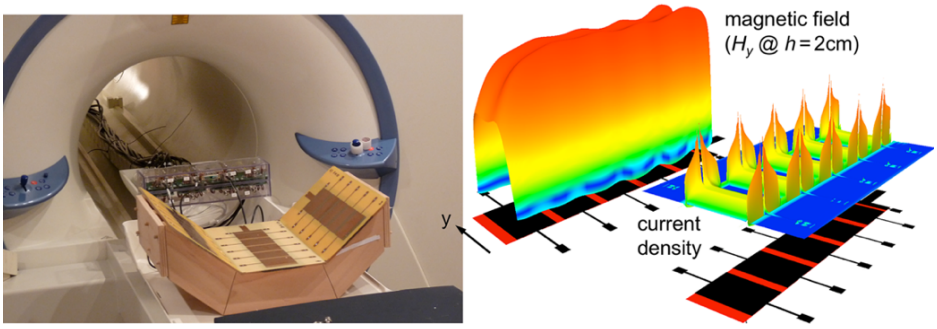

Figure 1. (left) CRLH ZOR coil element array; (right) FDTD simulations of the current density in the top metal layer and the resulting uniform $\boldsymbol{B}_1$ field distribution (H_y) 2cm above the metaline surface.

2.2. Dual-resonant coil elements for ^{23}Na/^{1}H 7T MRI

CRLH metalines are inherently dual-band due to the presence of both the right-handed and (folded) left-handed branch in the dispersion diagram. As shown in figure 2 a dual-band coil element has been realized based on a quarter-wave metaline resonator to target the Larmor frequencies of ^{23}Na and ^{1}H simultaneously for combined MRI at 7T [8, 9]. FDTD simulations provided (dimensionally adjusted) figures-of-merit $|\boldsymbol{B}_1^+|_{max}/(SAR_{max})^{0.5} = 2.7$dB (298MHz) and 12.2dB (79MHz) [8]. First MRI scanner experiments with fast gradient-echo sequences on a cylindrical phantom with 4 ping-pong ball insets (200/400mMol/l NaCl in water respective in agar) have revealed a distinct sodium selectivity mainly for the inset with 400mMol/l in agar, which is due to the low SNR/high coil losses at 79MHz [8].

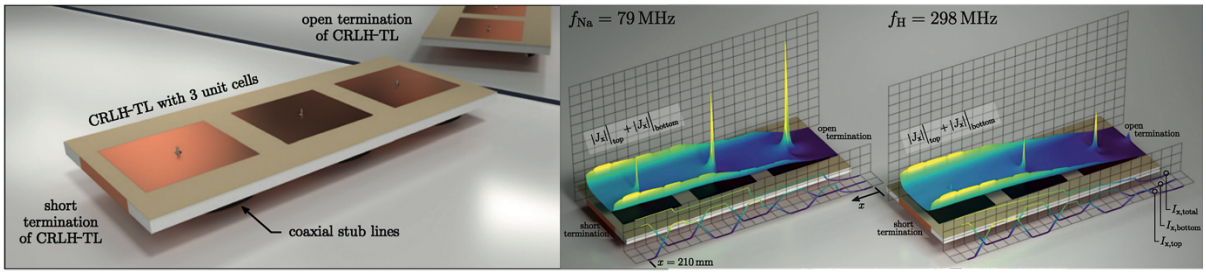

Figure 2. (left) Triple-layer MIM realization of the quarter-wave resonant CRLH dual-band coil element; (right) FDTD simulation of the combined current density on the top and bottom metal layer at the sodium frequency (79MHz) and the proton frequency (298MHz) with an equal λ/4 wave pattern.

2.3. Full-wave resonant ring antenna coils for 7T traveling-wave MRI

A full-wave resonance on a CRLH metaline, which is bent around to form a ring antenna (with 24 unit cells), provides a surface current distribution that has proven successful to excite the circularly polarized TE_{11} cylindrical waveguide mode within the context of traveling-wave MRI [10]. Using a longitudinally periodic arrangement of such ring antennas along the scanner bore allows – in the framework of an inverse problem solution for the excitation currents – for a distinct profiling of the $\boldsymbol{B}_1^+$ field along the patient's body. As displayed in figure 3 an accurate 15 cm wide profile (given the wavelength of the traveling waves of 3.6 m!) for *larynx* illumination has been achieved with a suppression of the unwanted $\boldsymbol{B}_1^-$ component (compared to $\boldsymbol{B}_1^+$) of 21dB while showing no SAR hot spots in the shoulder-neck region [11, 12]. It's worth noting that dispersion engineering underlying the CRLH ring antenna design allows the multiple ring antenna setting (i.e. the *MetaBore*) to fully conform to the inner surface of the cylindrical scanner bore providing an ergonomic as well as an electronically steerable «longitudinal shimming scheme» that may be conceptualized as an active cylindrical metasurface.

As proof-of-concept an in-vivo whole body 7T MRI study of a crab-eating macaque monkey has been carried out with a reduced setting of e.g. 2 CRLH ring antennas in Tx and Rx operation. Using FLASH (whole-body) and TSE (head) sequences well resolved images were retrieved with underlying $\boldsymbol{B}_1^+$ transmit efficiencies of 1.62μT/kW$^{0.5}$ (body) and 0.72μT/kW$^{0.5}$ (head) [13].

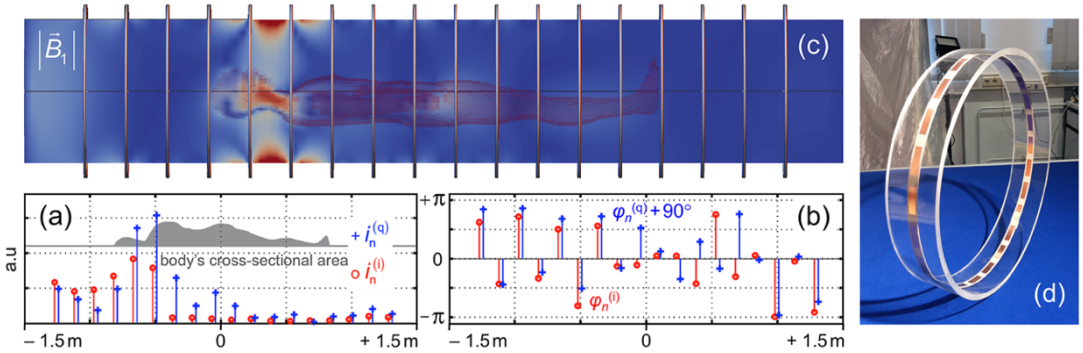

Figure 3. Simulated [18] traveling-wave profiling scenario for *larynx* illumination: (a) amplitudes and (b) phases of the 18 ring antenna's current excitations (width 1cm, pitch 15cm, diameter 64cm); (c) transversal RF magnetic field; and (d) CRLH ring antenna prototype (shown without ground plane); the body phantom is a cylindrically discretized version of *Duke*^{TM} from SPEAG's *Virtual Family*^{TM}.

3. Coils based on metamaterial high-impedance surfaces (HIS)

In order to enhance the uniformity and directivity of the RF magnetic field of e.g. elongated electric dipoles [15, 16] or series resonant loops [17] towards the probe volume, these coil elements were backed by an RF shield consisting of a 2D EM MTM (*metasurface*). The latter was realized as an uniplanar high-impedance surface (HIS) [14] where surface currents were efficiently suppressed yielding a realistic approximation to a perfect magnetic conductor (PMC). The rationale behind using HIS shields are the residual in-phase image currents that are in support of the currents in the overlaid coil elements providing an overall enhancement of the $\boldsymbol{B}_1$ field above the shielded coil. In this regard elongated dipole elements positioned 5mm over a HIS shield achieved a 26% enhancement of $\boldsymbol{B}_{1,\max}$ compared to a perfect electrical conducting (PEC) shield in addition to a 40% broadening of the cross-sectional field profile [15]. The resulting 8-channel HIS dipole coil design (cf. figure 4) was based on extensive FDTD analyses (using conformal meshing) [18] and provided an improved $\boldsymbol{B}_1$ homogeneity within a cylindrical phantom compared to a PEC shielded realization at the expense (as expected from the profile broadening) of a 3dB increased inter-element coupling [16].

4. Concluding remark

The aim of the presented work is to show that dispersion engineering in 1D and 2D EM metamaterials can provide additional degrees-of-freedom for multi-functional UHF MRI coil design along two con-

ceptual approaches; namely EM metalines as proper coil elements with tailored field distributions and/or multi-band features, and EM metasurfaces as additional measures for boosting MRI sensitivity.

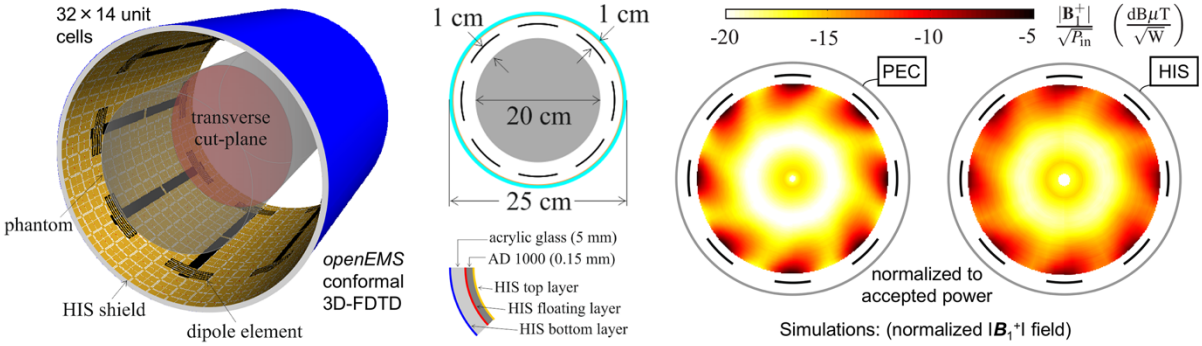

Figure 4. 8-channel HIS dipole coil: (left) FDTD simulation setup; (middle) coil dimensions with the simulated/experimental phantom; (right) simulated RF magnetic field (HIS vs. PEC ground planes).

Acknowledgments
We kindly acknowledge the Erwin L. Hahn Institute for Magnetic Resonance Imaging (ELH) of the university's hospital in Essen as well as at the Institute for Biometrics and Medical Informatics at the Otto-von-Guericke University in Magdeburg, both for their experimental support at their 7T MRI scanner systems (Siemens Magnetom).

References

[1] V. G. Veselago, *Sov. Phys. Usp.*, **10** (4), pp. 509-514, 1968.
[2] C- Caloz, *APSURSI 2016*, June 26- July 1, Fajardo, Puerto Rico, pp. 1299-1300, 2016.
[3] R. Schmidt, A. Slobozhanyuk, P. Belov, A. Webb, *Sci. Rep.*, **7** (1678), 2017.
[4] A. Rennings, J. Mosig, A. Bahr, C. Caloz, M. E. Ladd, D. Erni, *EuCAP 2009*, March 23-27, Berlin, pp. 3231-3234, 2009.
[5] A. Rennings, P. Schneider, C. Caloz, S. Orzada, *METAMATERIALS 2009*, Sept. 1-4, London, UK, pp. 126-128, 2009.
[6] A. Rennings, J. T. Svejda, K. Solbach, D. Erni, *MAGMA*, **26** (suppl 1), pp. 183-185, 2013.
[7] A. Rennings, J. Svejda, S. Otto, K. Solbach, D. Erni, *IEEE IMS 2013*, June 2-7, Seattle, USA, WE1E-1, 2013.
[8] J. T. Svejda, A. Rennings, D. Erni, *tm – Technisches Messen*, **84** (1), pp. 2-12, 2017.
[9] J. T. Svejda, D. Erni, A. Rennings, *MAGMA*, **29** (suppl 1), pp. S309, 2016.
[10] D. Erni, T. Liebig, A. Rennings, N. H. L. Koster, J. Froehlich, *33th IEEE EMBS 2011*, Aug. 30 - Sept. 3, Boston, MA, USA, pp. 554-558, 2011.
[11] H. Yang, T. Liebig, A. Rennings, J. Froehlich, D. Erni, *ICEAA 2013*, IEEE/URSI, Sept. 9-13, Torino, Italy, pp. 468-471, 2013.
[12] T. Liebig, J. T. Svejda, H. Yang, A. Rennings, T. Herrmann, J. Mallow, J. Bernarding, J. Froehlich, D. Erni, *ISMRM-ESMRMB 2014*, May 10-16, Milano, Italy, pp. 1358, 2014.
[13] T. Herrmann, *et al.*, *PLOS One*, **13** (1), paper e0191719, pp. 1-17, 2018.
[14] Z. Chen, K. Solbach, D. Erni, A. Rennings, *EuMC 2014*, Oct. 6-9, Rome, Italy, pp. 1576-1579, 2014.
[15] Z. Chen, K. Solbach, D. Erni, A. Rennings, *IEEE Trans. Microw. Theory Techn.*, **64** (3), pp. 972-983, 2016.
[16] Z. Chen, *Application of High Impedance Surfaces to Improve Radiofrequency Coil Performance for 7-Tesla Magnetic Resonance Imaging*, Ph.D. thesis, University of Duisburg-Essen, 2016.
[17] Z. Chen, K. Solbach, D. Erni, A. Rennings, *IEEE Trans. Microw. Theory Techn.*, **65** (3), pp. 988-997, 2017.
[18] T. Liebig, A. Rennings, S. Held, D. Erni, *Int. J. Numer. Model.*, **26** (6), pp. 680-696, 2013.